J Electroceram (2006) 17:287–292
DOI 10.1007/s10832-006-9436-9

Nanoscale phenomena of gallium-doped ZnO thin films on sapphire substrates

F. K. Shan · G. X. Liu · W. J. Lee · B. C. Shin · S. C. Kim

Received: 25 June 2005 / Revised: 16 May 2006 / Accepted: 12 June 2006

Abstract Gallium-doped ZnO (1.2 at. %) thin films with various thicknesses were deposited on sapphire (001) substrates at 500°C using a pulsed laser deposition (PLD) technique. The thin films with different thicknesses (20, 40, 100, 200, 400, and 600 nm, respectively) were obtained by changing the deposition time. An x-ray diffractometer (XRD) was used to investigate the structural properties of the thin films. All of the thin films had a preferred (002) orientation. However, the thin films with 20 and 40 nm thicknesses were of low crystallinity. With increasing thickness the (002) peak increased greatly, and the full width at half maximum (FWHM) values were calculated by using omega scans. Scanning electron microscope (SEM) and atomic force microscope (AFM) were used to investigate the nanoscale phenomena and the surface morphologies of the thin films. The surface roughness increased as the thickness increased. The thin film with 20 nm thickness was very smooth, and no nucleation center could be observed. However, the thin film with thickness over 100 nm showed nucleation. The nucleation center varied with increasing thickness. A spectrometer was used to investigate the luminescent properties of the thin films. It was found that all of the thin films showed near band edge emissions and no deep-level emissions were observed. A blueshift was also observed due to the Burstein-Moss effect.

Keywords ZnO · Thin film · XRD · SEM · AFM · Photoluminescence

F. K. Shan (✉) · G. X. Liu · W. J. Lee · B. C. Shin (✉)
Electronic Ceramics Center, DongEui University, Busan 614-714, South Korea
e-mail: fukaishan@yahoo.com

S. C. Kim
Department of Physics, DongEui University, Busan 614-714, South Korea

1 Introduction

As one of the versatile wide-band-gap semiconductors, ZnO has a lot of applications, especially in optoelectronic fields including gas sensors, surface acoustic wave devices, field effect transistors, and solar cells [1–4]. In recent years, much attention has been paid to its applications in blue and ultraviolet light emitting diodes (LEDs) and laser diodes (LDs) due to its wide band gap of 3.3 eV and large exciton binding energy of 60 meV at room temperature. Also, it is proven that GaN is a good material for the fabrication of optical devices, such as LEDs and LDs. The band structure and optical properties of ZnO are very similar to those of GaN, and the similarity in properties between ZnO and GaN makes ZnO one of the most promising materials for photonic devices in the ultraviolet range. Moreover, the binding energy of the exciton of ZnO (60 meV) is larger than that of GaN (25 meV) at room temperature. This is another advantage ZnO has over GaN for exciton-related device applications. As a result, ZnO-related materials have received considerable attention [5–9].

ZnO thin films had been grown by various techniques including sol-gel, chemical vapor deposition (CVD), molecule beam epitaxy (MBE), sputtering, and pulsed laser deposition (PLD) methods. Of these techniques, PLD is widely used in fabricating metal oxide thin films and the related materials because the plasma created by the pulsed laser is very energetic and its density is easily controllable by changing the experimental parameters. Its virtue is its simplicity and the atomic-layer control can be achieved by adjusting the laser fluence and the pulse rate. The processing of the multilayer heterostructure can be easily accomplished by using the multiple target carousels.

In the studies of ZnO thin films, most researchers reported that the PL spectra of ZnO samples showed a near-band-edge (NBE) UV emission line at around 379 nm accompanied by

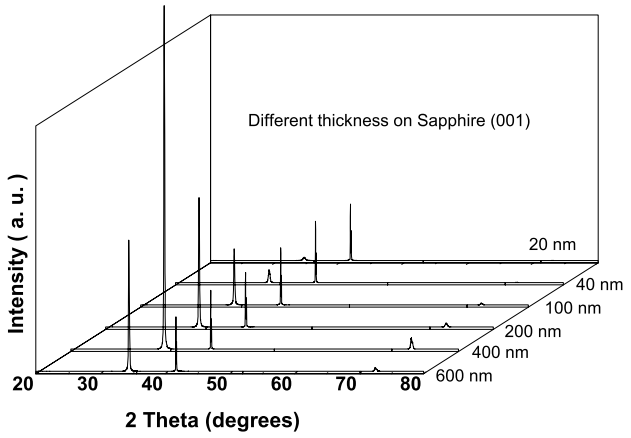

Fig. 1 XRD patterns of Ga:ZnO thin films with different thicknesses

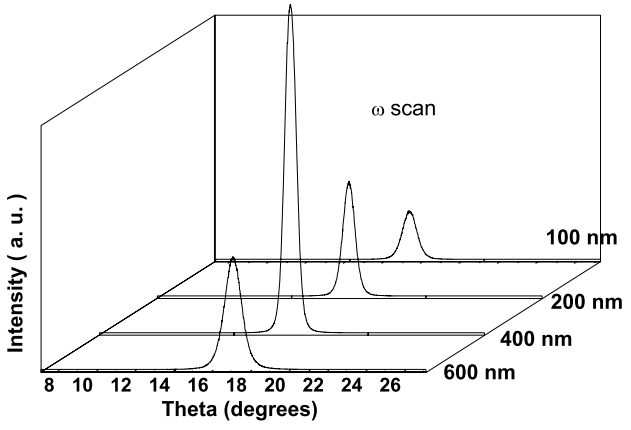

Fig. 2 Omega scans of Ga:ZnO thin films with different thicknesses

a broad deep-level (DL) luminescence, typically centered at around 500 nm, which can result in a decrease in carrier/exciton lifetime and emission efficiency in the UV light devices. This DL emission was observed in almost all ZnO epilayers grown on various substrates, including glass [10], sapphire [11, 12], silicon [13], and GaAs [14] by using CVD [11], MBE [15], PLD [16], and sputtering [13]. It appears that the DL emission from ZnO thin films is '*intrinsic*' in nature, and independent of the growth technique and substrates.

We have reported the aging effect of the PL spectra of ZnO thin films deposited using PLD. The aging effect demonstrated that the DL emission decreased as time went on [10, 14, 17]. It was experimentally proven that the DL emission in ZnO thin film deposited by PLD mainly originated from oxygen vacancies instead of zinc interstitials [18]. To decrease the DL emission in photonic devices, gallium dopant in ZnO thin films might be helpful in the decrease of DL emission. In this work, gallium-doped ZnO thin films (1.2 at.%) with various thicknesses were fabricated at 500°C on sapphire substrates using the PLD technique and their structural and optical properties were measured and discussed.

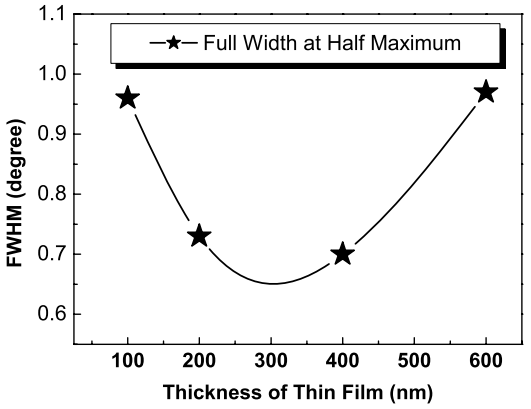

Fig. 3 FWHM values of (002) orientation of Ga:ZnO thin films with thicknesses of 50, 100, 200, and 300 nm

2 Experiment

In this experiment, PLD technique was used to deposit Ga-doped ZnO thin films (1.2 at.%) with various thicknesses on sapphire substrates. High-purity ZnO (99.99%) and Ga_2O_3 (99.99%) powder were used to make ceramic targets. To make the gallium-doped ZnO target, the desired amount of gallium powder was evenly mixed with ZnO powder in a planetary milling system for 24 hours using a plastic container without balls. A disk-shaped target was obtained by uniaxial pressing at 700 kg/cm^2, followed by a cold iso-static pressing at 24000 kg/cm^2. In order to produce a denser target, the disk-like target was sintered at 1200°C for 4 hours. The target was then attached to the target holder in the PLD chamber by epoxy resin. In our PLD system, a KrF excimer laser ($\lambda = 248$ nm, $\tau = 25$ ns) was used for the ablation of the target at an energy density of $\sim 2\ J/\text{cm}^2$. The strong absorption of 248 nm laser radiation by the target produced an intense plasma plume in front of the target surface. The ablated material was then deposited on a sapphire substrate held at 50 mm from the target. During thin film deposition the conditions were as follows: the repetition frequency of the laser was 5 Hz; the background O_2 pressure was 200 mTorr; and the substrate temperature was maintained at 500°C. The deposition time was 1, 2, 5, 10, 20, and 30 minutes. In this case the thickness of the thin film was about 20, 40, 100, 200, 400, and 600 nm, respectively. After deposition, the thin films were cooled naturally to room temperature for various measurements.

The crystalline structures of the thin films were studied by an x-ray diffractometer (XRD, D/MAX 2100H, Rigaku, Japan, 40 kV, 30 mA) using CuKα1 radiation with $\lambda = 1.5405$ Å. The nanoscale phenomena and relaxation of the thin film with different thicknesses were investigated by a field-emission scanning electron microscope (FE-SEM, HITACHI S-4200, Hitachi Co.). The surface morphologies of the thin films were investigated by a scanning probe

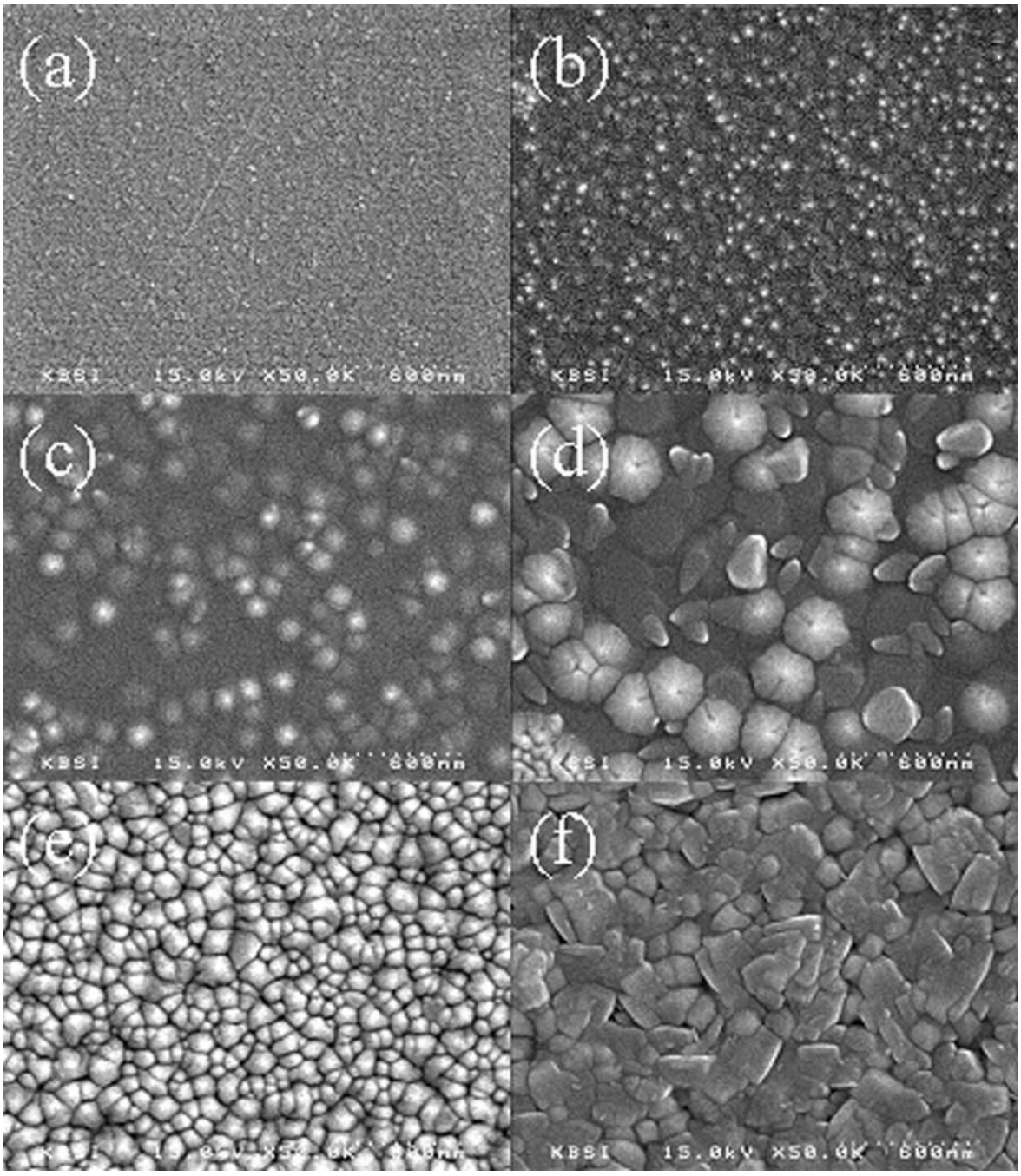

Fig. 4 SEM images of Ga:ZnO thin films with thicknesses of 20 nm (a), 40 nm (b), 100 nm (c), 200 nm (d), 400 nm (e), and 600 nm (f)

microscope (SPA-400, Seiko Instrument, Japan) in the AFM mode. The excitation source used for the measurements of their luminescent properties was a He-Cd laser operating at 325 nm with an output power of 50 mW. The emitting light from the sample was focused into the entrance slit of a monochromator that had a spectral grating of 1200 grooves/mm. This was picked up by a photomultiplier tube. A cutoff filter was used to suppress the scattered laser radiation. The cutoff wavelength of the filter at the ultraviolet side was about 340 nm.

3 Results and discussion

Figure 1 shows XRD patterns of gallium-doped ZnO (Ga:ZnO) thin films with various thicknesses on sapphire (001) substrates deposited at 500°C using PLD. It was found that, except for the sapphire (006) peak, Ga:ZnO (002) orientation was observed in all of the thin films. However, the peak intensity of Ga:ZnO (002) orientation greatly depended on the thickness of the film. The peak intensity of Ga:ZnO (002) orientation increased with increasing thickness up to

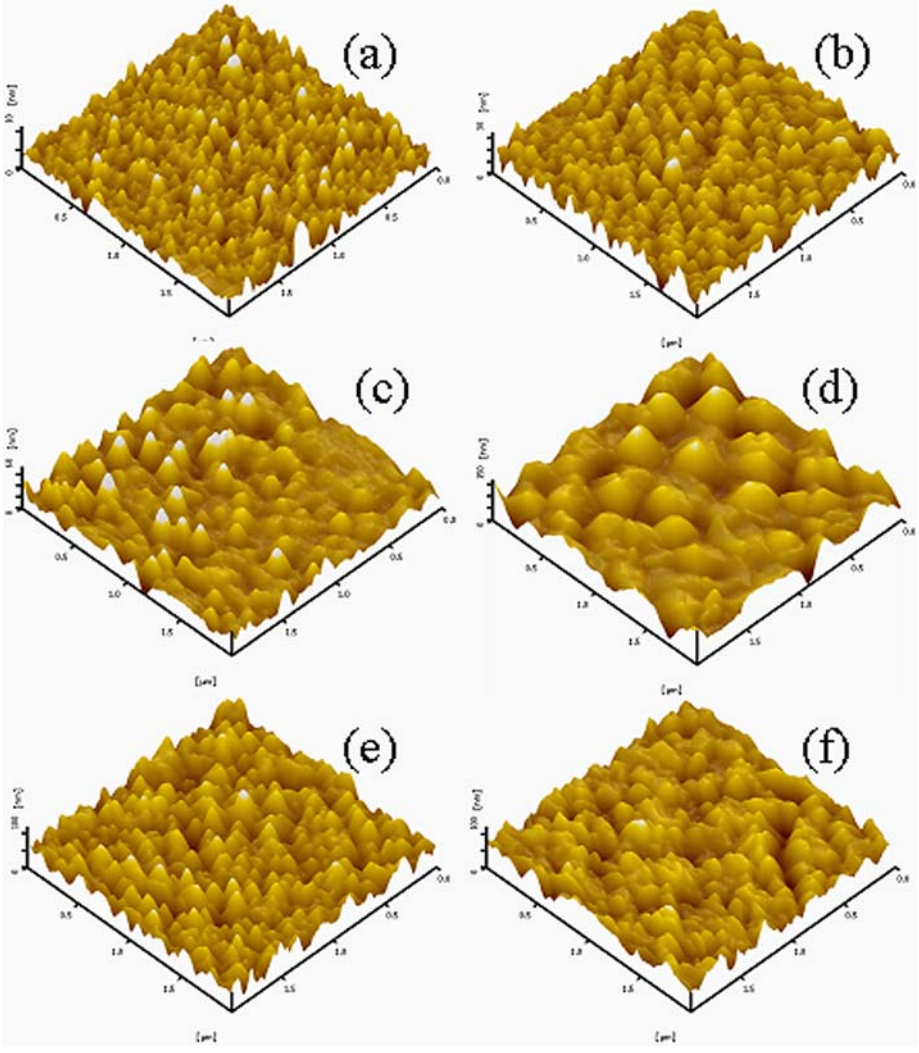

Fig. 5 AFM images of Ga:ZnO thin films with thicknesses of 20 nm (a), 40 nm (b), 100 nm (c), 200 nm (d), 400 nm (e), and 600 nm (f)

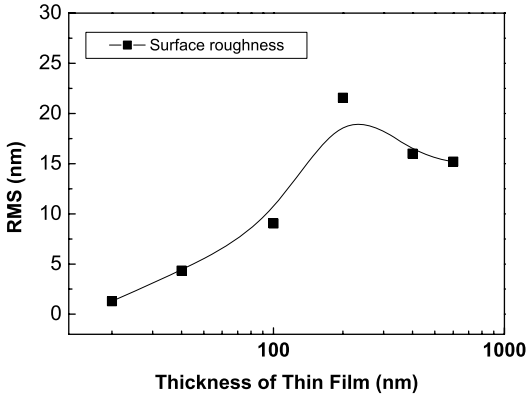

Fig. 6 Surface roughness of Ga:ZnO thin films with different thicknesses

400 nm. This is due to the increase of the thickness and the improvement of the crystal structure. However, the peak intensity of Ga:ZnO (002) orientation of the 600 nm-thick film decreased. This decrease in intensity may be due to the distortion of the crystal structure, which can be verified by the omega scan.

Figure 2 shows the omega scans of the Ga:ZnO thin films with thicknesses of 100, 200, 400, and 600 nm, respectively. Note that it was very difficult to measure the omega scans for the thin films with the thicknesses of 20 nm and 40 nm. To evaluate the crystal quality of the thin film, the full width at half maximum (FWHM) values were calculated and were shown in Fig. 3. It was found that the FWHM values were 0.97°, 0.73°, 0.7°, and 0.97°, respectively, for the thin films with thicknesses of 100, 200, 400, and 600 nm. The thin films with thicknesses of 200 nm and 400 nm were of higher crystalline quality compared to the others. This means that the crystal quality of the thin film may be improved while the thickness of the thin film increased up to 400 nm. However, the FWHM value of (002) orientation of 600 nm-thick film increased up to 0.97°. This is evidence that the thickness is important in determining the crystal quality.

Figure 4 shows the SEM surface images of Ga:ZnO thin films with various thicknesses on sapphire (001) substrates deposited at 500°C using PLD. Figure 4(a) shows the SEM

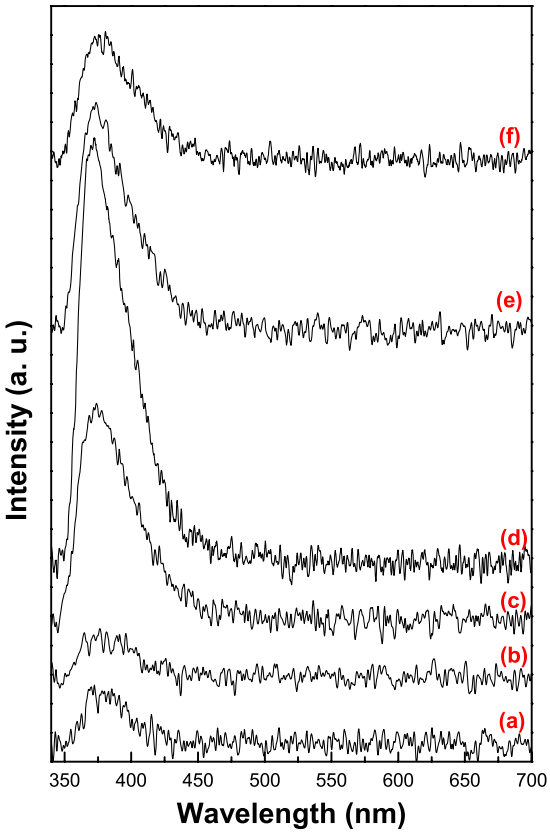

Fig. 7 PL spectra of Ga:ZnO thin films with different thicknesses

image of Ga:ZnO thin film with thickness of 20 nm. It can be seen that the surface was very smooth and homogeneous. In this step, the growth is layer-by-layer and a layer is completely filled before the next layer starts to grow. With increasing the thickness up to 40 nm, as shown in Fig. 4(b), a lot of nucleation centers (islands) were observed on the thin film. However, all of the nucleation centers were very small. As the thickness of the thin film increased, the size of the nucleation centers increased gradually and the number of nucleation center decreased. Several nucleation centers emerged into one. The film with the thickness of 200 nm were of the largest grain size, which was around 200 nm in diameter. For the Ga:ZnO film with a thickness thinner than 200 nm, the boundaries among the grains were very loose.

As the thickness of the film continually increased up to 400 nm, the number of nucleation centers increased again and the size of the nucleation centers decreased to around 50–100 nm in diameter. It seems that the 400 nm-thick film is the most compact, which can be observed in the cross-section SEM images of the film (not shown here). This revealed that Ga:ZnO film with 400 nm thickness was composed of well-aligned columns grown vertically on the sapphire substrate. The diameter of the column was about 50–100 nm. However, the film with 600 nm thickness changed a lot in the size and the shape of the grain. The size increased again and the grain changed from a round-like shape to a tetragon-like shape. From the SEM images of all of the thin films, the surface of the thin film with a thickness of 400 nm was the most homogeneous. The SEM images indicated that the film growth mechanism changed from layer-by-layer growth mode to island growth mode.

To quantitatively measure the surface roughness of the thin films deposited with various thicknesses, the surface morphologies of the thin films were measured by an SPA-400 in the AFM mode and were shown in Fig. 5. Figure 5(a), (b), (c), (d), (e), and (f) show the AFM images of Ga:ZnO thin films with thicknesses of 20, 40, 100, 200, 400, and 600 nm, respectively. The grain size varying with thickness was clearly observed by AFM measurements. The root mean square (RMS) values were 12.9, 43.5, 90.5, 215.2, 160.0, and 152.0 Å for the thin films with thicknesses of 20, 40, 100, 200, 400, and 600 nm, respectively. The RMS values were plotted and shown in Fig. 6. It was found that the 20 nm-thick film was very smooth and the grain size was the smallest. With increasing thickness, the surface tends to be rougher and the RMS roughness increased by as much as one order of magnitude from 12.9 Å for 20 nm-thick film to 90.5 Å and 215.2 Å for the 100 nm and 200 nm thick film, respectively. With further increase of the thickness, the RMS value of Ga:ZnO film tends to be maintained at around 150–160 Å.

Figure 7 shows the PL spectra of Ga:ZnO films with various thicknesses on sapphire (001) substrates deposited at 500°C using the PLD technique. According to our previous results [10], the PL spectrum of pure ZnO thin film usually showed two emission peaks. One was the near band edge (NBE) emission and the other was the deep-level (DL) emission. However, Mg-doped ZnO thin film showed an NBE emission peak only, which had a blueshift compared to pure ZnO due to the Burstein-Moss effect. Also no DL emission peak was observed in Mg-doped ZnO thin film. From Fig. 7, it was also observed that Ga:ZnO thin film showed only one NBE emission peak and no DL emission was observed. The NBE emission peak of Ga:ZnO thin film was located at about 372 nm, which had a blueshift compared to the PL of pure ZnO (379 nm). This blueshift was believed to originate from the Burstein-Moss effect.

4 Conclusions

In summary, gallium-doped ZnO (1.2 at. %) thin films with various thicknesses (20, 40, 100, 200, 400, and 600 nm) were deposited on sapphire (001) substrates at 500°C using the PLD technique. XRD showed that all of the films had a preferred Ga:ZnO (002) orientation. However, the thin films with 20 and 40 nm thicknesses were of low crystallinity.

With increasing thickness the (002) peak increased greatly. The FWHM values were measured by the omega-scan to investigate the crystal quality. A scanning electron microscope and an atomic force microscope were used to investigate the nanoscale phenomena and the surface roughnesses of the thin films. The surface evolution was clearly observed, and the surface roughness increased with increasing thickness. The thin film with 20 nm thickness was very smooth, and no nucleation center could be observed. However, the thin film with a thickness over 100 nm showed nucleation. The nucleation center increased with increasing thickness. Luminescent properties of the thin films revealed that all of the thin films showed NBE emissions and no deep-level emission. A blueshift due to the Burstein-Moss effect was observed compared to the PL of pure ZnO.

Acknowledgments This work is supported by Electronic ceramics center at DongEui University as an RIC program of ITEP under MOCIE and Busan Metropolitan City.

References

1. T.L. Yang, D.H. Zhang, J. Ma, H.L. Ma, and Y. Chen, *Thin Solid Films*, **326**, 60 (1998).
2. B. Sang, A. Yamada, and M. Konagai, *Jpn. J. Appl. Phys.*, **37**(Part 2), L206 (1998).
3. P. Verardi, N. Nastase, C. Gherasim, C. Ghica, M. Dinescu, R. Dinu, and C. Flueraru, *J. Crystal Growth* **197**, 523 (1999).
4. J.F. Cordaro, Y. Shim, and J.E. May, *J. Appl. Phys.*, **60**, 4186 (1986).
5. Y.R. Ryu, S. Zhu, J.D. Budai, H.R. Chandrasekhar, P.F. Miceli, and H.W. White, *J. Appl. Phys.*, **88**, 201 (2000).
6. D.C. Look, *Mater. Sci. Eng. B*, **80**, 383 (2001).
7. F.K. Shan, B.C. Shin, S.C. Kim, and Y.S. Yu, *J. Eur. Ceram. Soc.*, **24**, 1861 (2004).
8. F.K. Shan, G.X. Liu, B.I. Kim, B.C. Shin, S.C. Kim, and Y.S. Yu, *J. Korean Phys. Soc.*, **42**, S1157 (2003).
9. Y.F. Lu, H.Q. Ni, Z.H. Ni, Z.H. Mai, and Z.M. Ren, *J. Appl. Phys.*, **88**, 498 (2000).
10. F.K. Shan, B.I. Kim, G.X. Liu, Z.F. Liu, J.Y. Sohn, W.J. Lee, B.C. Shin, and Y.S. Yu, *J. Appl. Phys.*, **95**, 4772 (2004).
11. S. Bethke, H. Pan, and B.W. Wessels, *Appl. Phys. Lett.*, **52**, 138 (1988).
12. H.T. Ng, B. Chen, J. Li, J. Han, and M. Meyyappan, *Appl. Phys. Lett.*, **82**, 2023 (2003).
13. S.H. Jeong, B.S. Kim, and B.T. Lee, *Appl. Phys. Lett.*, **82**, 2625 (2003).
14. F.K. Shan, Z.F. Liu, G.X. Liu, W.J. Lee, G.H. Lee, I.S. Kim, B.C. Shin, and Y.S. Yu, *J. Electroceram.*, **13**, 195 (2004).
15. H.J. Ko, T. Yao, Y.F. Chen, and S.K. Hong, *Appl. Phys. Lett.*, **76**, 1905 (2000).
16. F.K. Shan, B.C. Shin, S.W. Jang, and Y.S. Yu, *J. Eur. Ceram. Soc.*, **24**, 1015 (2004).
17. F.K. Shan, G.X. Liu, W.J. Lee, G.H. Lee, I.S. Kim, B.C. Shin, and Y.C. Kim, *J. Crystal Growth*, **277**, 284 (2005).
18. F.K. Shan, G.X. Liu, W.J. Lee, G.H. Lee, I.S. Kim, and B.C. Shin, *Appl. Phys. Lett.*, **86**, 221910 (2005).